Dalton Transactions

PAPER

View Article Online
View Journal

Cite this: DOI: 10.1039/c5dt04011f

Copper(I) complexes with phosphine derived from sparfloxacin. Part II: a first insight into the cytotoxic action mode†

U. K. Komarnicka,[a] R. Starosta,[a] M. Płotek,[b] R. F. M. de Almeida,[c] M. Jeżowska-Bojczuk*[a] and A. Kyzioł*[b]

Received 13th October 2015,
Accepted 1st December 2015

DOI: 10.1039/c5dt04011f

www.rsc.org/dalton

In this paper we present a first insight into the cytotoxic action mode of copper(I) iodide or copper(I) thiocyanate complexes with a phosphine derivative of sparfloxacin (a 3rd generation fluoroquinolone antibiotic agent) and 2,9-dimethyl-1,10-phenanthroline or 2,2′-biquinoline as auxiliary ligands. The *in vitro* cytotoxic activity of the new complexes was tested against two cancer cell lines (CT26 – mouse colon carcinoma and A549 – human lung adenocarcinoma). An ICP-MS study revealed a marked time-dependent intracellular copper accumulation of the tested compounds. In addition, confocal microscopy imaging showed accumulation of the complexes inside whole cells and their emission of blue light. The complexes generate reactive oxygen species in the cancer cells, which was examined by using two different fluorescent probes. Moreover, (i) DNA intercalation studied by luminescence spectroscopy, circular dichroism and molecular docking, and (ii) plasmid DNA damage also demonstrate their significant cytotoxicity. All these observed biological effects contribute to the induction of apoptosis, observed at a great predominance.

Introduction

In recent years the number of reports on the synthesis, design and development of copper(I) complexes has significantly increased.[1] They have been tested for antibacterial,[2] antiviral,[3,4] antifungal[5] and anti-inflammatory[6] activities. However, such complexes are mostly interesting as anticancer agents.[1,7–12] In general, copper complexes are supposed to be less toxic to normal cells with respect to tumour cells. It is mainly explained by the specific physiological properties of copper as an endogenous metal.[13,14] In particular, coordination compounds containing S-donor and/or phosphine ligands seem to be the best candidates for clinical trials, because of their proven cytotoxicity against cancer cells and high stability in aqueous solutions.[1]

Despite numerous literature reports concerning *in vitro* and *in vivo* cytotoxic activities of the various Cu(I) complexes, rather scarce studies on the precise mechanism of their cytotoxic effects have been published so far.[15–17] Nevertheless, the published data suggest that the cytotoxic mechanism of copper complexes is different from that of platinum and ruthenium drugs.[1,16,17] It is mainly based on copper redox activity and affinity for binding to sites occupied by other metals. Also, recent mechanistic studies indicate the signalling pathways involved in paraptosis.[13–15] Thus, copper complexes offer a new possibility to overcome apoptosis-resistance of cancer cells. Moreover, it is proposed that the alleged cell targets of the copper(I) coordination compounds are topoisomerases and complex multi-protein proteasomes.[1,12,18] Most likely, Cu(I) complexes have inhibitory properties on these enzymes, which may result in the cancer cell death. Besides, it is also speculated that the action mechanism of the above-mentioned complexes may be associated with their ability for DNA intercalation.[19] Summing up, the determination of the specific mechanism leading to tumour cell death is necessary for the rational design of anticancer therapeutics.

In our previous paper[20] we presented the synthesis, physicochemical properties and cytotoxicity of the new copper(I) iodide and copper(I) thiocyanate complexes with **PSf** – a phosphine derived from sparfloxacin (**HSf**), a 3rd generation quinolone and selected diimines as auxiliary ligands (see Fig. 1). We used 2,9-dimethyl-1,10-phenanthroline (dmp) and 2,2′-biquinoline (bq), which are characterised by high steric hindrances. Therefore, they successfully prevent the tetrahe-

[a]Faculty of Chemistry, University of Wrocław, F. Joliot-Curie 14, 50-383 Wrocław, Poland. E-mail: malgorzata.jezowska-bojczuk@chem.uni.wroc.pl
[b]Faculty of Chemistry, Jagiellonian University, R. Ingardena 3, 30-060 Kraków, Poland. E-mail: kyziol@chemia.uj.edu.pl
[c]Centro de Química e Bioquímica, Departamento de Química e Bioquímica, Faculdade de Ciências, Universidade de Lisboa, Campo Grande, 1749-016 Lisboa, Portugal

†Electronic supplementary information (ESI) available. See DOI: 10.1039/c5dt04011f

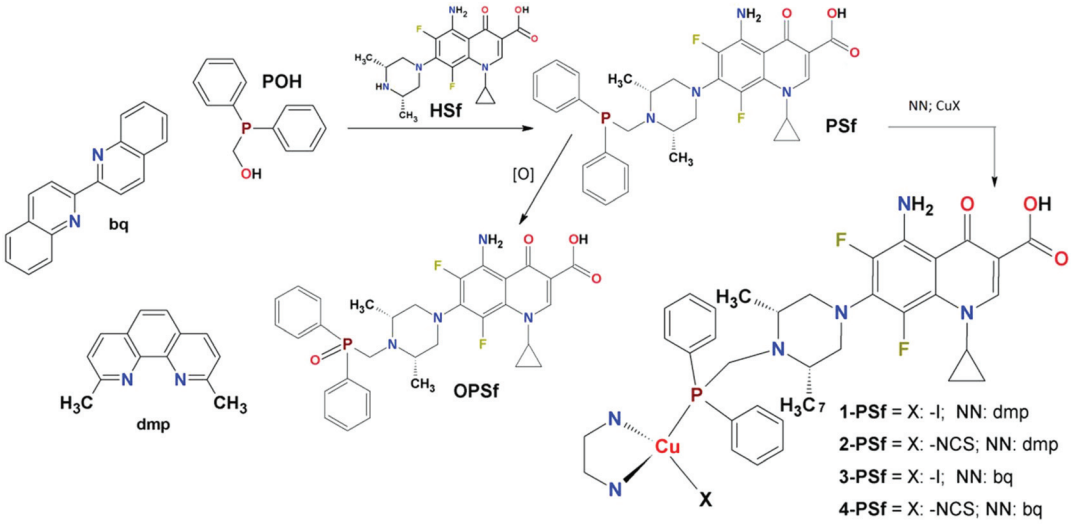

Fig. 1 Schematic view of the investigated compounds' synthetic route.

dral geometry around the copper centre from flattening upon excitation leading usually to oxidation from Cu(I) to Cu(II).[7,9,21–24] We have also shown that all the synthesized complexes are characterised by a high stability in an aqueous environment which resulted not only from the presence of dmp or bq, but also from the stable Cu–I or Cu–NCS bonds, as proven by the lack of the formation of $Cu(NN)_2^+$ species (NN: dmp or bq) in solution.[20] Four complexes (see Fig. 1) with the **PSf** ligand ([CuI(dmp)PSf] – **1-PSf**, [CuNCS(dmp)PSf] – **2-PSf**, [CuI(bq)PSf] – **3-PSf** and [CuNCS(bq)PSf] – **4-PSf**), characterized by a significantly high cytotoxic activity were selected for more detailed studies presented in this paper.

Herein we try to approach the mechanism of cytotoxic action towards the CT26 cell line (mouse colon carcinoma, morphology: fibroblast, ATCC: CRL-2638) and A549 cell line (human lung adenocarcinoma, morphology: epithelial, ATCC: CCL-185) of the aforementioned complexes. To realize our goal we undertook a series of experiments: (i) the mode of cell death was examined by flow cytometric analysis, (ii) intracellular uptake of the tested complexes was studied by ICP-MS spectrometry and confocal microscopy, (iii) the ability of the complexes to generate reactive oxygen species (ROS) in the cells was examined using two different fluorescent probes (cyto-ID hypoxia/oxidative stress detection kit and H2DCF-DA), (iv) interactions of complexes with DNA were investigated using luminescence spectroscopy, circular dichroism and molecular docking as well as (v) generation of DNA plasmid degeneration was studied by gel electrophoresis.

Results and discussion

Stability in a biological system

The stability of the studied complexes in DMEM solution (see definition in the Experimental section) was examined using UV-Vis spectroscopy (see Fig. 2). For all complexes, their characteristic charge transfer absorption band (MX,MPR3) LCT[9,25] did not disappear during 48 h of experiments, similarly to the results obtained in pure water with DMSO.[20] This is clear evidence of the absence of Cu(I) to Cu(II) oxidation processes under aerobic conditions in the medium.

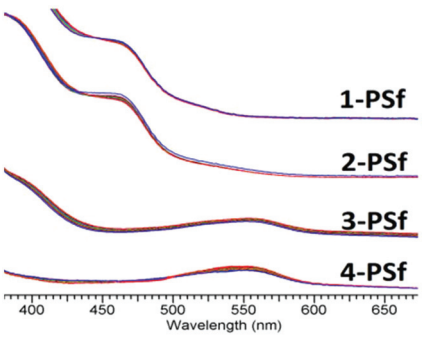

Fig. 2 Stability of the investigated complexes during 48 h in DMEM with 2% DMSO.

Mode of cell death

In our previous paper we presented the cytotoxic activity of the studied complexes and ligands against A549 and CT26 cell lines.[20] The determined values of IC_{50} (the half maximal inhibitory concentration) for selected compounds are summarised in Table 1. Cell viability was additionally observed using fluorescence imaging microscopy by staining with fluorescein diacetate (FDA) and propidium iodide (PI).[20] The obtained results however did not allow us to distinguish between apoptotic and necrotic cellular death.

For more precise determination of the mode of observed cell death we applied flow cytometry with Fluorescence-Acti-

Table 1 IC_{50} values [μM] for CT26 and A549 cell lines after 4 and 24 h treatment with the copper(I) complexes and free ligands[20]

	IC_{50} [μM] ± SD			
	4 h		24 h	
	CT26	A549	CT26	A549
HSf	255.20 ± 13.52	273.50 ± 10.63	122.84 ± 4.21	201.53 ± 12.14
PSf	238.97 ± 16.76	163.23 ± 5.08	264.28 ± 12.07	104.08 ± 3.30
OPSf	51.03 ± 1.21	74.90 ± 1.43	109.23 ± 8.76	52.72 ± 9.23
1-PSf	7.33 ± 0.06	6.04 ± 0.03	8.29 ± 0.71	7.84 ± 0.16
2-PSf	7.75 ± 0.19	7.02 ± 0.02	7.88 ± 0.58	7.51 ± 0.34
3-PSf	24.52 ± 1.02	24.70 ± 2.50	9.32 ± 0.42	8.25 ± 0.08
4-PSf	42.64 ± 0.73	23.99 ± 1.21	33.79 ± 8.08	9.06 ± 0.47

vated Cell Sorting (FACS). For this, an Annexin V/PI assay was performed and the apoptosis-inducing ability of the tested copper complexes (**1-PSf**, **2-PSf**, **3-PSf** and **4-PSf**) and also with organic compounds (**HSf**, **PSf** and **OPSf**) was quantitatively evaluated. At an early stage of apoptosis the flipped phosphatidylserine of the cytoplasmic membrane becomes available on the cell surface for binding to Annexin V. Together with propidium iodide (PI), which stains only dead cells with a disintegrated membrane, Annexin V enables distinguishing cells undergoing different types of cell death. The percentage of live, early and late apoptotic as well as necrotic cells upon treatment with the complexes (IC_{50}) is presented in Fig. 3 (CT26 line treated with the complexes) and in the ESI (see Fig. S1–S10 and Table S1†).

Detailed data analysis showed that treatment of the cells with all the tested compounds resulted in the population of apoptotic cells appearing, while the necrotic ones were present in minority. This is particularly evident in the case of **1-PSf** and **3-PSf** complexes possessing an iodide ligand (see Fig. 3A and C). Substitution of this ligand for a thiocyanate one led to remarkable stimulation of necrotic cell death (**2-PSf** and **4-PSf**, see Fig. 3B and D). Both described effects were better seen after a shorter incubation time (4 h) for both the tested cell lines. It can be supposed that diimine ligands (dmp, bq) have less impact on the type of cell death, since the percentage of apoptotic and necrotic cells for complexes **1-PSf** and **2-PSf** as well as for **3-PSf** and **4-PSf** is at the comparable level for both incubation times (compare Fig. 3A and B with Fig. 3C and D). However, at this stage of investigation, taking into account that 24 hours of incubation with the studied compounds resulted in a similar population of necrotic cells for **3-PSf** and **4-PSf**, it cannot be clearly concluded with an identifiable impact of the ligand on the type of cell death.

Cellular uptake

In an attempt to correlate cytotoxicity with the cellular uptake of the tested compounds, the copper content was evaluated for CT26 cells treated for 4 and 24 h with **1-PSf**, **2-PSf**, **3-PSf** and **4-PSf** with IC_{50} concentration. The intracellular copper amount was quantified by ICP-MS analysis and is expressed as ng Cu per mg of cellular protein (see Fig. 4).

Treatment of CT26 cells with the tested copper complexes resulted in a marked time-dependent intracellular copper accumulation. After 4 h of incubation with all the compounds, an almost twenty-five fold increase of copper complex accumulation was detected over control cells (see Fig. 4 and Table S2†). Despite different starting concentrations of the tested compounds in the medium (IC_{50}, see Table 1), after

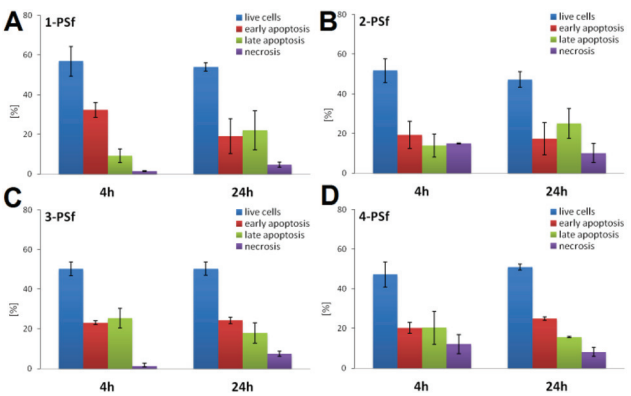

Fig. 3 Percentage [%] of normal, apoptotic and necrotic cells after 4 and 24 h of incubation of CT26 cell line with complexes: (a) **1-PSf** (b) **2-PSf**, (c) **3-PSf** and (d) **4-PSf** in IC_{50}.

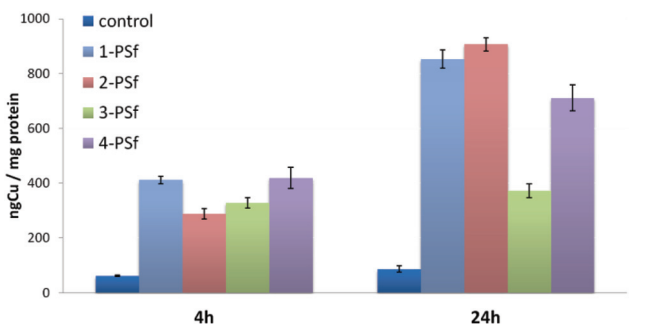

Fig. 4 Final intracellular copper concentration expressed by ng Cu per mg protein after 4 and 24 h of incubation with cancer line CT26 for complexes **1-PSf**, **2-PSf**, **3-PSf** and **4-PSf** in IC_{50}.

4 hours of incubation the resulting Cu level in the cells was comparable for the complexes with the dmp ligand (**1-PSf** and **2-PSf**) and complexes with bq (**3-PSf** and **4-PSf**). It indicates that dmp complexes are characterised by a greater capacity for copper accumulation inside cells. Whereas, longer incubation (24 h) resulted in a further, significant increase of the copper accumulation *i.e.* approximately 2-fold increase for **1-PSf** and **4-PSf** and about 3-fold increase for **2-PSf**. Importantly, no significant difference in metal accumulation with an increased incubation time was detected for **3-PSf**. One can suppose that compounds which enter better and faster inside the cell, probably should show enhanced cytotoxic properties. In our particular case, it was observed that the duration of the incubation time importantly influenced the accumulation level of metal complexes. This indicates that the studied complexes should exhibit changeable cytotoxicity within time; however, this was clearly seen only in the case of **3-PSf** and **4-PSf** compounds. In contrast to these complexes, **1-PSf** and **2-PSf** ones did not show this kind of relationship (see Fig. 4 and Table S2†), despite a strong correlation between incubation time and copper complex uptake. At this stage of investigation it can be supposed that for better activity, **3-PSf** and **4-PSf** compounds require a longer incubation time and thus it also presumably indicates a different mechanism for their action. From the observed correlation between the type of diimine ligand and the level of copper complex accumulation inside cells, it may be stated that the mode of action of these compounds depends probably on their accumulation rate.

These conclusions encourage clarification of the mechanisms for the cellular uptake of the synthesized compounds. Further studies would reveal whether the type of ligand determines efficient and fast uptake and observed cytotoxicity. Nevertheless, other variables, such as the ability for DNA intercalation or induction of ROS production, are also involved in the observed cytotoxicity of the studied complexes. These will be discussed in the next part of this work.

Luminescent microscope and confocal imaging

Analysis of intracellular accumulation of anticancer agents is the next, important step to understand the mechanism of their action.[26] The application of confocal microscopy in our study was possible because of the luminescence properties of the ligands as well as the described copper(I) complexes.

HSf, its derivatives (**PSf** and **OPSf**) and complexes are characterised by an intense luminescence of the –Sf fragment in solution (Fig. 5C). The maximum of the emission band for all of these compounds is located around 500–540 nm. Interestingly, for the **1-PSf** and **2-PSf** complexes there is a second, lower energy band with a maximum observed around 590–600 nm. This band may be a result of MLCT transition typical for the emission spectra of the $[CuX(dmp)PR_3]$ complexes.[21,22] Charge transfer emission for such types of complexes is however observed only in the solid state. In the solution, due to the high flexibility of the complexes resulting in the flattening deformations from the tetrahedron in the excited state, a non-radiative relaxation path is followed back to the ground state.[27] The unexpected presence of the MLCT band for **1-PSf** and **2-PSf** is most probably a result of the high steric hindrances of the –Sf moiety in the **PSf** ligand.

After 4 h incubation of all the tested compounds with the tumour cells, photos of the cells in visible light and upon excitation at 358 nm were obtained using a luminescence microscope (see Fig. 5A). The treated cells were characterised by an intense blue emission (see Fig. 5A4), in contrast to the control ones (see Fig. 5A2). The luminescence spectra of the compounds in the cells were additionally recorded using a spectrophotometer coupled with a luminescence microscope (see Fig. 5B). Due to the low intensity of the spectra, detailed analysis of the band maxima was not possible. However, ligands and the complexes with the bq ligand were characterised by one emission band, while in the spectra of the dmp complexes accumulated in cancer cells, two bands were clearly seen. It is worth to emphasise that the spectra of the compounds inside

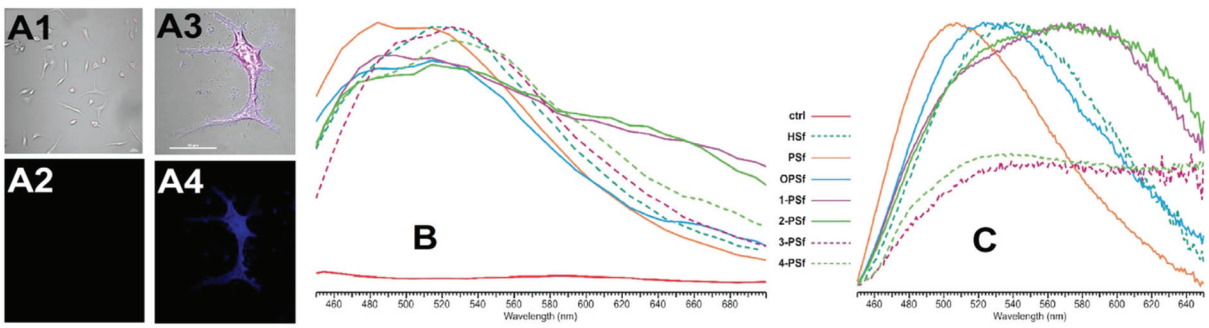

Fig. 5 Fluorescence emission of the compounds in cells and in buffer solution. (A) Cancer cell (A549) 1: without complexes (magnification 40.00×, bar 10 μm) in visible light, 2: without complexes (40.00×, bar 10 μm), λ_{ex} = 358 nm, 3: with **1-PSf** complex treated with an IC_{50} dose for 4 h in visible light (60.00×, bar 20 μm), 4: with **1-PSf** complex treated with an IC_{50} dose for 4 h; λ_{ex} = 358 nm (60.00×, bar 20 μm). (B) Emission spectra of accumulated compounds in A549 cells after 4 h incubation with an IC_{50} dose and control cells (λ_{ex} = 358 nm), obtained with a fluorescence microscope coupled to a spectrometer, ctrl – control. (C) Normalized emission spectra of the studied compounds (in PBS buffer with 2% of DMSO; *c* = 210–5 M) obtained in cuvette measurements with a spectrofluorometer. Spectra of **3-PSf** and **4-PSf** (characterized by low luminescence) were divided by 2.

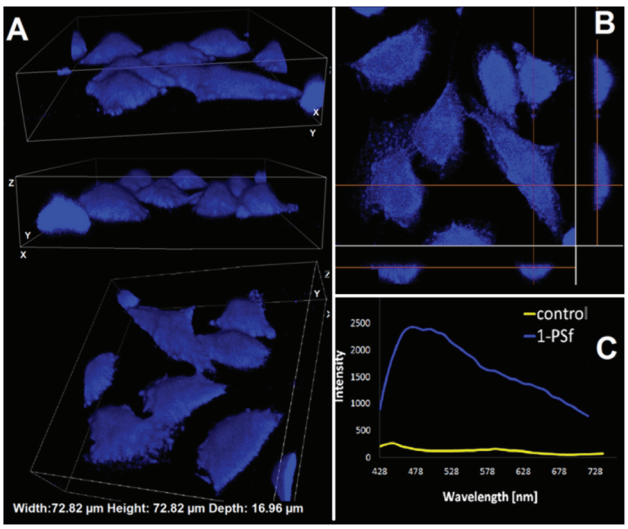

Fig. 6 (A) Selected 3D photos of A549 cells in different positions obtained by confocal microscopy (magnification 60.00×, bar 10 µm; ex = 358 nm) after 4 h incubation with **1-PSf** (in IC_{50}) together with an (B) cross-sectional image. (C) Emission spectrum of cells after treatment with **1-PSf** (IC_{50}), ex = 358 nm and the control ones.

a cell are in good agreement with the spectra recorded in a buffer solution despite completely different experimental configurations and the different environment of the molecules. Moreover the obtained results indicate the presence of **1-PSf** and **2-PSf** in the cell and are a direct proof of the high stability of these complexes.

Confocal microscopy was used to confirm and visualise the penetration of the investigated complexes into the tumour cells. In addition, this method allowed us to determine the intracellular location of the studied compounds. For this purpose, suitable preparations (Experimental section) were carried out and the cells were incubated with the tested compounds (IC_{50}) for 4 h. In general, the obtained images for all the compounds were comparable. Selected data for the **1-PSf** complex are presented in Fig. 6. Analysis of the cross-sectional images and emission bands of cancer cells proved unequivocally that the tested compounds penetrate into the cells, and there were no favourable locations inside the cell where the compounds accumulated. Emission from the compounds was visible inside the whole cell. In addition, in the obtained pictures, there were no locations of varying intensity, which indicated that the compounds were uniformly distributed throughout the cells (see Fig. 6).

Reactive oxygen species (ROS) production

It is known that apoptosis or cell cycle arrest, mediated *inter alia* by metal complex treatment, is associated with ROS production.

Any oxidative damage to the constituents of the mitochondrial respiratory chain, caused among others by metal ions, may lead to uncoupling of the mitochondrial respiration. This allows a subsequent transfer of electrons to molecular oxygen, present inside the cell. In consequence this leads to the mitochondrial $O_2^{\bullet -}$ and H_2O_2 formation in a positive feedback mode. Indeed, mitochondrial ROS production is a very early indication before the breakdown of mitochondrial membrane potential, which in turn results in releasing the pro-apoptotic factors or the activation of the other cell death mechanisms.[1,10–13]

Cellular ROS production in A549 and CT26 cells upon 4 and 24 h treatment with **1-PSf**, **2-PSf**, **3-PSf** and **4-PSf** (IC_{50}) was monitored by H2DCF-DA, the fluorescent ROS probe. In addition, the level of oxidative stress induced by the total ROS production was also determined using a cyto-ID hypoxia/oxidative stress detection kit. As positive controls: H_2O_2 and pyocyanin were used in the first and second cases, respectively.

Our studies have proved that the investigated complexes as well as free ligands displayed the ability to induce ROS production inside the treated cells (see Fig. 7 and Fig. S11–S14†). Both the performed tests showed that all the studied complexes and the corresponding ligands were able to induce ROS generation at a similar level and independently of the type of cell line (see Fig. S11–S14†). The lack of a strong correlation between ROS production and compound structure suggests that ROS are probably not primarily involved in the observed cytotoxicity and the mechanism of cell death. More precise experiments will help to explain their special contribution and kind of participation in the observed cytotoxicity.

Moreover, since we observed significant differences in the IC_{50} values during the first 4 hours of incubation with the studied compounds (IC_{50}: **1-PSf**, **2-PSf** > **3-PSf**, **4-PSf**) and there is no significant difference in the accumulation rate for all the complexes (*vide supra* see Table 1 and Fig. 3, 4), it can be supposed that the cytotoxic mechanism during this four first hours of incubation is different.

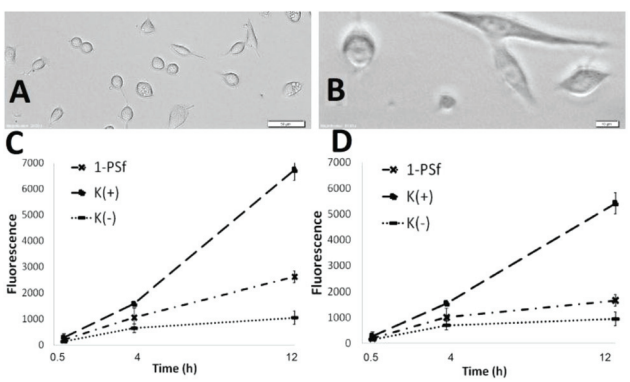

Fig. 7 Photos of CT26 cells after 4 h treatment with **1-PSf**. (A) – magnification 20.00×, bar 50 µm (B) – magnification 40.00×, bar 10 µm; (C) the increase of ROS production in CT26 cells after 30 min, 4 and 12 h using H_2DCF-DA for: **1-PSf**, K(+): H_2O_2 as the positive control and K(–): negative control, cell without compounds; (D) oxidative stress induced by the total ROS production in CT26 cells after 30 min, 4 and 12 h detected by the CYTO-ID Hypoxia/Oxidative Stress Test for: **1-PSf**, K(+): pyocyanin as the positive control and K(–): negative control.

In vitro interactions with CT DNA

Most drugs tend to interact with DNA noncovalently through three selective modes: (i) a groove-bound fashion stabilised by a mixture of hydrophobic, electrostatic and hydrogen-bonding interactions; (ii) an intercalative association with planar, heteroaromatic moieties between the DNA base pairs; and (iii) electrostatic binding.[28–30] More and more often it has been speculated that the mechanism of cytotoxic action of copper(I) compounds may be associated with their ability for DNA intercalation.[1,12,18] Since the complexes discussed here are characterised by a high stability in water[20] or medium and possess in their molecules an aromatic diimine[31] and a fluoroquinolone moiety of undoubtedly intercalating ability,[32–36] a deeper insight into that interaction mechanism might be an important factor for a better understanding of their therapeutic efficacy. We studied the possible interactions of the investigated compounds with calf thymus DNA (CT DNA), which is widely used in examinations of DNA binding agents. The most popular technique for investigation of the mode of interactions involves competitive experiments using the ethidium bromide (EB) complex with CT DNA. EB is a typical indicator forming intercalation complexes, which emit intensive fluorescence.[37–40] The compound that can bind more strongly than EB decreases the DNA-EB emission, due to the replacement of EB and/or electron transfer.[41,42]

The emission spectra of EB bound to CT DNA were recorded in the presence of increasing amounts of the investigated ligands and complexes according to a literature method.[43] All the compounds were predissolved in DMSO, which did not influence the CT DNA–EB complex solution in the volumes used (see Fig. S15†). The addition of compounds resulted in a significant decrease of the intensity of the CT DNA–EB characteristic emission band (see Fig. S16–S19†). The Inner Filter Effect was included and the corrected intensity of emission was calculated using eqn (1)[44] where Abs is the absorbance at the analysed emission wavelength, I_f is the uncorrected emission intensity.

$$I_{cor} = \frac{I_f \ 2.303\,Abs}{(1 - 10^{-Abs})} \quad (1)$$

The competition reaction that takes place between intercalating compounds and DNA-bound EB is not a true quenching process, because there is no direct interaction between EB and the compounds. Rather, the much lower quantum yield of free EB accounts for the observed decrease in fluorescence intensity. However, the fact that all the Stern–Volmer plots (see Fig. 8) have good or fair linearity (R^2 = 0.94 for **HSf**, 0.85 for **PSf**, 0.90 for **OPSf**, 0.79 for **1-PSf**, 0.83 for **2-PSf**, 0.96 for **3-PSf** and 0.86 for **4-PSf**) suggests that these can be used as an empirical description of the data, and to qualitatively compare the intercalating ability of the studied compounds.

The strength of the ligands' interaction with DNA formed the following order: **HSf** > **OPSf** > **PSf**. The results showed that the **HSf** derivation drastically lowered its intercalating ability. It is worth noting that our data are comparable with those

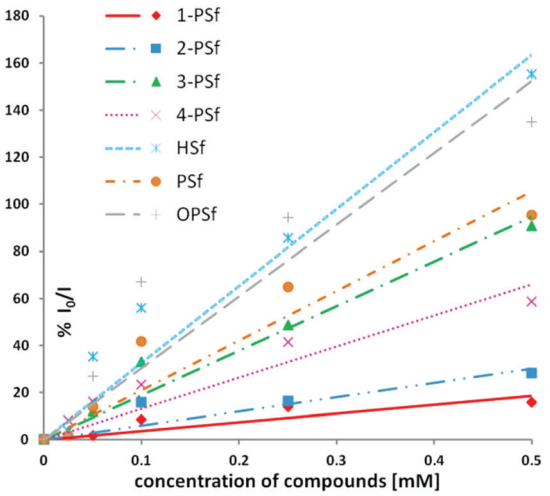

Fig. 8 Stern–Volmer plots of the CT DNA–EB system quenched by **HSf**, **PSf**, **OPSf**, **1-PSf**, **2-PSf**, **3-PSf** and **4-PSf**; (I_0 and I – intensity of CT DNA–EB in the absence and presence of the increasing concentration [mM] of the compounds.

obtained for **HSf** in aqueous solution, where a twenty-fold excess of sparfloxacin resulted in an 80% decrease of the CT DNA–EB luminescence intensity.[40] Whereas, for the complexes, the strength of intercalations formed the following order: **3-PSf** > **4-PSf** ≫ **2-PSf** > **1-PSf**, showing the decisive influence of a diimine ligand. The bq complexes are significantly more efficient intercalators than the dmp ones, regardless of the pseudo(halide) anion (see Fig. 8 and S16–S19†).

Circular dichroism (CD) spectroscopy is *inter alia* used to characterise the binding of the small molecules to the DNA and its conformational changes. The CD spectra of CT DNA exhibit a positive Cotton effect at 275 nm due to the base stacking, and a negative one at 245 nm due to the helical character, typical for the B form of DNA.[45] After CT DNA titration by **HSf**, **PSf** and **OPSf**, bands on all spectra did not show noticeable changes, contrary to the complexes. This means that copper complexes affected the DNA structure, while organic compounds did not (see Fig. S17 and S19†).

Molecular docking

In order to test the groove binding mode and DNA intercalating potential of the studied compounds, we investigated their interactions with the double-stranded (ds) helical DNA. We employed several fragments of various DNA structures, which let us obtain some general results and avoid accidental errors. For the groove binding studies we used two different oligonucleotides: an optimised synthetic canonical B form of the DNA ds hexadecanucleotide ("BETA", ATATCGCGATATCGCG, see Fig. 9A and B) and DNA ds dodecanucleotide (PDB ID 423D, ACCGACGTCGGT, see Fig. 9C and D).[46] The first of these sequences was used by us previously to study DNA interactions with the derivatives of ciprofloxacin and norfloxacin and their copper complexes.[47] The second one was successfully

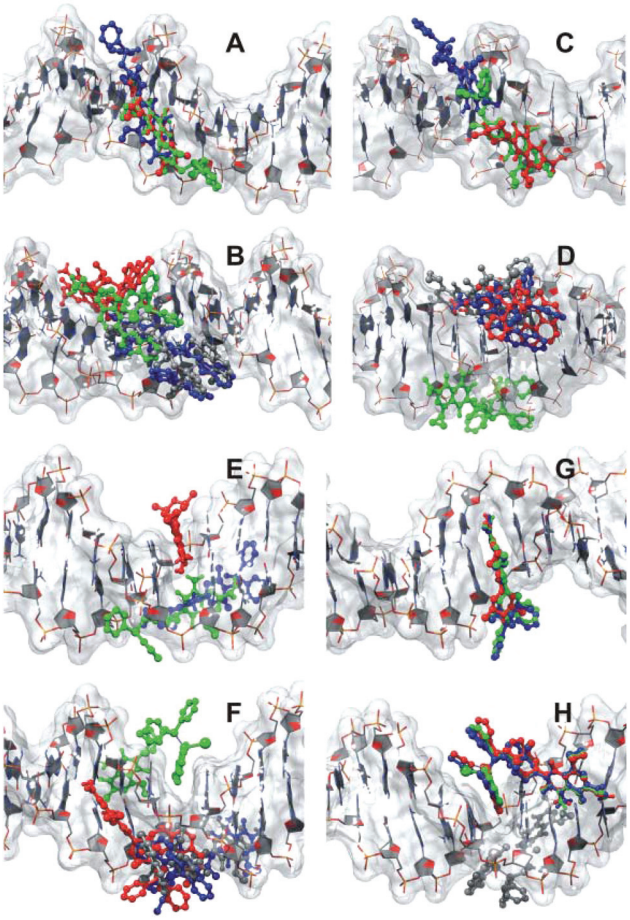

Fig. 9 Lowest energy conformers of **HSf**, **PSf** and **OPSf** (red, green and blue, respectively; A, C, G, E) as well as the copper complexes **1-PSf**, **2-PSf**, **3-PSf** and **4-PSf** (dim grey, red, green and blue, respectively; B, D, H, F) docked to helical "BETA" (A, B) and 423D (C, D) DNA structures and the DNA structures with the predefined intercalation gaps ("TA" – E, F and "GC" – G, H).

employed by Vijayakrishna to study groove binding of an imidazolium-based polyelectrolyte.[48] For the analysis of the intercalation potential we used two different optimised structures of the ATATCGCGATATCGCG ds hexadecanucleotide with preformed intercalating gaps between the 6th and 7th base pairs ("GC" gap, see Fig. 9E and F) or between the 10th and 11th base pairs ("TA" gap, see Fig. 9G and H).[47]

The geometries of the studied compounds were calculated using the DFT methods. For all organic ligands possessing the sparfloxacin moiety we optimised the structures with methyl substituents on the piperazine ring in the equatorial positions (as found in the X-ray structures of **HSf**[19] and **OPSf**[49]). While for the complexes, the structures with the corresponding methyl substituents in the axial positions were examined.[20] The qualitative analysis of the docking results was based on the lowest energy poses for each molecule. The binding free energies [kcal mol^{-1}] of the lowest energy conformers with the comments for all the tested compounds are given in Table 2. Moreover, Tables S3 and 4 in the ESI† contain all the obtained data.

Data analysis of the interactions with helical "BETA" and 423D DNA structures shows that organic ligands tend to bind to the minor groove, while the Cu(I) complexes bind to the major one (**3-PSf** interactions with 423D is the only exception, see Fig. 9D). In each case the binding is determined by a set of hydrogen bonds between nucleotides and pyridone oxygen as well as $-NH_2$ and –COOH groups of the sparfloxacin moiety. Binding free energy analysis shows clearly that the interaction strength is the lowest for **HSf** and the highest for **OPSf** ligands regardless of the type of helix. Among the complexes, the ones with the dmp ligand bind more strongly than the bq ones (also except **3-PSf**) (see Table 2).

A study of the intercalation potential of the tested compounds gives an interesting picture. For both synthetic structures ("TA" and "GC") partial intercalation was preferable only for free **HSf** and the bq complexes (**3-PSf**, **4-PSf**), which are characterised by the higher groove binding energies. However in the case of "GC" structure, almost all the compounds (except **1-PSf**) demonstrate their ability to partially intercalate the DNA structure. Moreover, in all cases of intercalation, compounds are located at the major groove.

Summing up, the obtained results show strong groove binding and moderate intercalation ability for the discussed

Table 2 Groove binding and intercalation energies [kcal mol^{-1}] for all studied compounds

Energy [kcal mol^{-1}]								
Groove binding					Intercalation			
	"BETA"		423D		"TA"		"GC"	
HSf	−7.1	mng	−7.4	mng	−7.1	pi *via* –COOH and $-NH_2$ (mjg)	−8.0	pi *via* –COOH and $-NH_2$ (mjg)
PSf	−8.1	mng	−8.1	mng	−8.1	mng (ni)	−8.1	mng (ni)
OPSf	−8.2	mng	−8.9	mng	−8.3	mng (ni)	−8.3	mng (ni)
1-PSf	−8.4	mjg	−8.9	mjg	−8.4	mng (ni)	−8.5	mng (ni)
2-PSf	−8.4	mjg	−8.9	mjg	−8.4	mng (ni)	−8.0	mng (ni)
3-PSf	−8.2	mjg	−9.2	mng	−9.1	pi *via* diimine (mjg)	−8.9	pi *via* diimine (mjg)
4-PSf	−8.2	mjg	−8.7	mjg	−8.4	mng (ni)	−9.0	pi *via* diimine (mjg)

mng – minor groove, mjg– major groove, pi – partial intercalation, ni – no intercalation.

compounds. This confirms the results of the spectroscopic studies and proves that molecular docking can be regarded as a complementary technique and can clarify spectroscopic results.

Generation of plasmid DNA damage

In many cases, anticancer drugs that intercalate into DNA can cause its breakage.[50] The studied compounds intercalated to DNA, hence investigation of generation of DNA damage is of great importance.

The gel electrophoresis of pBR322 plasmid (naturally occurring as a covalently closed superhelical form (form I)) was applied to determine the ability of **HSf**, **PSf**, **OPSf** and complexes **1-PSf**, **2-PSf**, **3-PSf**, **4-PSf** to induce single- and/or double-strand damage to DNA. This can lead to the formation of the relaxed/nicked (form II) and linear (form III) forms. It should be emphasised that **HSf**, which proved in our study to be the strongest DNA intercalator, as well as **PSf** and **OPSf**, did not cause any DNA degradation (see Fig. S20†), even in concentrations exceeding the IC_{50} (500 μM) in contrast to the complexes (see Fig. 10). The degree of DNA degradation was determined in a wide range of concentrations (from 10 to 500 μM) (see Fig. S21, S22 and Tables S5, S6†), and a densitometry analysis was performed as well (see Fig. 11). With the increase of each complex's concentration, the extent of the nicked form and/or linear ones increased, which proves single- and/or double cleavage.

Dmp complexes caused only single-strain plasmid damage. As is clearly seen in Fig. 11, **1-PSf** led to the formation of form II in larger amounts (see Fig. S21† lines 2–7) than **2-PSf** (see Fig. S21† lines 8–13), in the same concentrations. This means that **1-PSf** interacted more strongly with DNA. It is worth noting that bq complexes caused not only single-, but also double-strain plasmid cleavage (see Fig. S22† **3-PSf** lines 4–6 and **4-PSf** lines 10–12). Form III appeared in the same concentration (100 μM) for both of them. After densitometric analysis it is easy to see that **4-PSf** generated higher amounts of linear form in comparison with **3-PSf** (see Fig. 11).

In the presence of transition metal ions and their complexes, an endogenous oxidant H_2O_2 could be a source of hydroxyl radicals, the most powerful DNA oxidants.[51] The

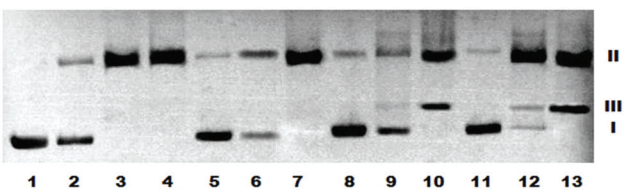

Fig. 10 Agarose gel electrophoresis of pBR322 plasmid cleavage by copper(I) complexes in a DMF (each in the 10% DMF) solution. Lanes: 1, plasmid – control; 2, plasmid + 10 μM **1-PSf**; 3, plasmid + 100 μM **1-PSf**; 4, plasmid + 500 μM **1-PSf**; 5, plasmid + 10 μM **2-PSf**; 6, plasmid + 100 μM **2-PSf**; 7, plasmid + 500 μM **2-PSf**; 8, plasmid + 10 μM **3-PSf**; 9, plasmid + 100 μM **3-PSf**; 10, plasmid + 500 μM **3-PSf**; 11, plasmid + 10 μM **4-PSf**; 12, plasmid + 100 μM **4-PSf**; 13, plasmid + 500 μM **4-PSf**.

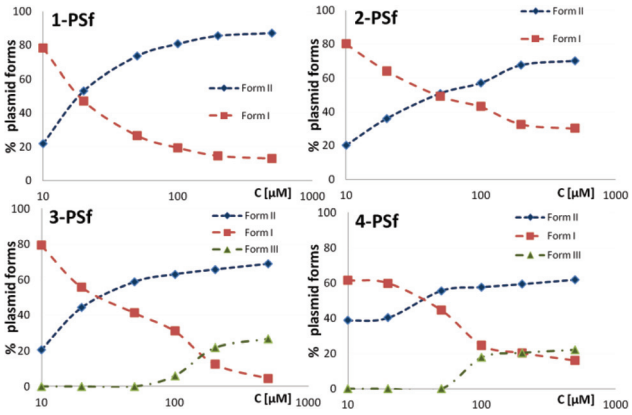

Fig. 11 Densitometric analysis of plasmid cleavage by **1-PSf**, **2-PSf**, **3-PSf** and **4-PSf** (*X* axis: concentration [μM] on a logarithmic scale; *Y* axis: % plasmid forms).

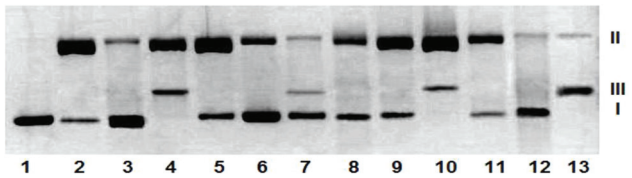

Fig. 12 Agarose gel electrophoresis of pBR322 plasmid cleavage by copper(I) complexes in a DMF(each in the 10% DMF) solution. Lanes: 1, plasmid + 10% DMSO; 2, plasmid + 50 μM **1-PSf**; 3, plasmid + 50 μM **1-PSf** + 10% DMSO; 4, plasmid + 50 μM **1-PSf** + 50 μM H_2O_2; 5, plasmid + 50 μM **2-PSf**; 6, plasmid + 50 μM **2-PSf** + 10% DMSO; 7, plasmid + 50 μM **2-PSf** + 50 μM H_2O_2; 8, plasmid + 50 μM **3-PSf**; 9, plasmid + 50 μM **3-PSf** + 10% DMSO; 10, plasmid + 50 μM **3-PSf** + 50 μM H_2O_2; 11, plasmid + 50 μM **4-PSf**; 12, plasmid + 50 μM **4-PSf** + 10% DMSO; 13, plasmid + 50 μM **4-PSf** + 50 μM H_2O_2.

studied complexes probably decomposed H_2O_2 in a free radical reaction, which can cause additional DNA damage. The investigated coordination compounds under these conditions caused distinct changes in the plasmid structure, resulting in conversion of the supercoiled plasmid to a linear form (see Fig. 12 lines 4, 7, 10 and 13). Very interesting and worth mentioning is the fact that the addition of DMSO (effective scavenger of the hydroxyl free radical[52]) to the reaction's mixture affected DNA damage (see Fig. 12 lines: 4, 7, 10 and 13). Prevention of double lesions by DMSO confirmed a free radical mechanism of action on the plasmid degradation processes[9,53] (see Fig. 12 lines 3, 6, 9 and 12).

Experimental section

Cell culture

CT26 cell line (mouse colon carcinoma, morphology: fibroblast, ATCC: CRL-2638) and A549 cell line (human lung adenocarcinoma, morphology: epithelial, ATCC: CCL-185) were cultured in Dulbecco's Modified Eagle's Medium (DMEM)

without phenol red, supplemented with 10% foetal bovine serum (FBS) and with 1% streptomycin/penicillin. Cultures were incubated at 37 °C under a humidified atmosphere containing 5% CO_2 (standard conditions). Cells were passaged at preconfluent density, using a solution containing 0.05% trypsin and 0.5 mM EDTA.

Cell cycle analysis using flow cytometry

In order to distinguish cell death induced by **1-PSf**, **2-PSf**, **3-PSf** and **4-PSf** complexes, Annexin V Apoptosis Detection Kit APC (Affymetrix) was used. The studied compounds (IC_{50}) were incubated for 4 or 24 h with tumour cells (density 500 000 cells per mL) in 12-well plates. After this time, the compound solutions were removed and the cells were washed with PBS (phosphate-buffered saline, pH = 7.4) buffer and binding buffer. Trypsin was added to the cells and then they were left for 10 min at 37 °C under a humidified atmosphere containing 5% CO_2. The cells were collected, centrifuged and separated from the supernatant, then washed with 0.5 ml PBS buffer (phosphate-buffered saline: NaCl, KCl, Na_2HPO_4, KH_2PO_4) and again centrifuged and separated from the supernatant. Finally, 5 μl fluorochrome-conjugated Annexin V was added to the cells before they were resuspended in 0.5 mL binding buffer. Such prepared samples were incubated at room temperature for 15 min. Then, the cells were centrifuged, separated from the supernatant and washed with 0.5 mL binding buffer. Afterwards, the cells were again centrifuged, resuspended in 0.5 ml binding buffer and 5 μL propidium iodide staining solution was added. Measurements using a flow cytometer (FACSCalibur Becton, Dickinson and Company) were carried out after 30 min; the samples were stored in the dark. The experiment was repeated at least 3 times. The dot-plots of the percentage distribution of individual cell populations were obtained.

Copper uptake

Cells at a density of 2 000 000 cells per 2 mL were seeded in 6-well plates and were incubated with **1-PSf**, **2-PSf**, **3-PSf** and **4-PSf** complexes in IC_{50} for 4 or 24 h. After this time, compound solutions were removed and the cells were washed twice with PBS buffer. The cells were trypsinized. Then, they were washed twice with PBS buffer. Cells for ICP-MS analysis were mineralised in 1 mL of 65% HNO_3. Measurement of the concentration of copper ions was carried out using a mass spectrometer (ELAN 6100 Perkin Elmer) with an inductively coupled plasma (ICP-MS). The protein content was assessed with the Bradford Protein Assay (Thermo Scientific™).[14] The copper content under each condition is expressed as ng Cu per mg protein. The experiment was repeated at least 3 times.

Luminescence microscopy and confocal imaging

Confocal laser scanning microscopy (CLSM Nikon) was used to visualise the intracellular accumulation of **HSf**, **PSf**, **OPSf**, **1-PSf**, **2-PSf**, **3-PSf** and **4-PSf** complexes. Cells were seeded on coverslips at a density of 500 000 per mL in 9-well plates and left for 24 h for adhesion to the bottom. The growth medium was replaced with a medium containing **HSf**, **PSf**, **OPSf**, **1-PSf**, **2-PSf**, **3-PSf** or **4-PSf** in IC_{50}. The cells were incubated for 4 h at 37 °C under a humidified atmosphere containing 5% CO_2. After this time the cells were washed twice with PBS buffer. Cells were fixed by treating for 30 min with 2.5% glutaraldehyde (PBS buffer solution) at room temperature. After this time the cells were washed twice with PBS buffer. Afterwards, the cells were left for 30 min in an increasing concentration gradient of ethanol (20, 40, 60, 80 and 99%). Then, the cells (on coverslips) were washed twice with PBS buffer and covered by microscope slides. The samples were directly imaged under a Nikon A1 confocal laser scanning system (CM) attached to an inverted microscope Nikon Ti (Japan). A 1009 objective lens (Nikon Plan Apo VC/1.40 oil) was used. The samples were excited with diode lasers (405 and 488 nm). Fluorescence spectra were collected using a 32-channel spectral detector.

Fluorescence measurements of the compounds in aqueous buffer

Steady-state fluorescence measurements were carried out on a Spex Fluorolog® 3-22 spectrofluorometer from Horiba Jobin Yvon at room temperature (23 ± 2 °C) with double grating monochromators in both excitation and emission light paths. For these measurements, the final compound concentration was 20.0 μM in PBS buffer with 2% of DMSO. Semi-micro fluorescence cuvettes from Hellma® were used. The spectra of the pure mixture of solvents were recorded for appropriate background correction. For acquisition of the emission spectra of the compounds, excitation was performed at 370 nm. Bandwidth was 5 nm in both excitation and emission.

Reactive oxygen species (ROS) production

Production of Reactive Oxygen Species (ROS) by **1-PSf**, **2-PSf**, **3-PSf** and **4-PSf** compounds was determined by photometric tests using: 5-(and-6)-chloromethyl-20,70-dichlorodihydrofluorescein, diacetate acetyl ester (H2DCF-DA) and a Cyto-ID® Hypoxia/Oxidative Stress Detection Kit. The assay was performed in 96-well plates, where the cells were seeded at a density of 10 000 cells per 0.2 mL of medium. Acetyl ester (H2DCF-DA) was prepared by dissolving it in sterile DMSO under anaerobic conditions. Next, the dye solution was diluted in a medium with 2% serum. The medium from the cells was removed, and they were also washed using PBS buffer. Dye solution at a final concentration of 1 μM was added. Cells with the dye were incubated for 30 min in the dark (37 °C under a humidified atmosphere containing 5% CO_2). After this time the dye solution was removed and the cells were washed twice with PBS buffer. Solutions of the studied complexes in IC_{50} and a solution of H_2O_2 (final concentration −100 μM) as a positive control were added to the cells. The cells with the investigated substances were incubated for 30 min, 4 and 12 h at 37 °C under a humidified atmosphere containing 5% CO_2. The emission of solution was measured at 495 nm using an Infinite 200M PRO NanoQuant plate reader (Tecan, Switzerland). The results obtained using acetyl ester (H2DCF-DA) were confirmed by the results obtained using a second dye Cyto-ID® Hypoxia/Oxidative Stress Detection Kit. In this case, the

cells were incubated with the tested compounds for 30 min, 4 and 24 h at 37 °C under a humidified atmosphere containing 5% CO_2. After 3.5 h of incubation, a ROS-inducing reagent as a positive control was added to the untreated cells. After 4 h all supernatants were removed, the cells were washed twice with PBS buffer and Oxidative Stress Detection Kit was used. The cells with the dye were incubated under standard conditions for 1 h. After this time the emission spectra with an excitation wavelength of 505 nm was recorded. The experiment was repeated at least 3 times. The results were presented as a graph of emission intensity, which is proportional to ROS concentration at an appropriate point of time.

Interaction of the compounds with calf thymus DNA

The stock solution was prepared by dissolving CT DNA in 50 mM phosphate buffer saline (PBS) (pH = 7.4). The CT DNA concentration (c = 2.66 × 10^{-3} M) was determined by using a UV spectrophotometer using the molar absorption coefficient 6600 M^{-1} cm^{-1} at 258 nm. The stock solution was stored at 4 °C and used for not more than 5 days. A luminescent complex of CT DNA with EB (ethidium bromide) was prepared by mixing of substrates in an equimolar ratio (c(CT DNA–EB) = 5 × 10^{-5} M; 50 mM of the phosphate buffer at pH = 7.4). The solution of the CT DNA–EB system was titrated in different molar ratios (0.5, 1, 2, 5 and 10) by **HSf**, **PSf**, **OPSf**, **1-PSf**, **2-PSf**, **3-PSf** and **4-PSf** (dissolved in DMSO) and incubated for 1 h with any portion of each of the investigated compounds. Photoluminescence measurements were recorded at 298 K on a Cary Eclipse fluorescence spectrophotometer. Excitation wavelength was equal to 510 nm. The spectra of circular dichroism were recorded using a spectropolarimeter JASCO J-715 (CD and MCD).

Molecular docking

The structures of the ligands (organic molecules and copper complexes) were optimised using the GAUSSIAN 09 package.[54] We employed the DFT method using the hybrid functional of Truhlar and Zhao[55] (M06). The basis set employed for geometry optimisation calculations was: 6-31G* for all atoms (except I: 6-311G** [56,57]).

The DNA models for docking were prepared according to the following procedure. The initial configuration of the canonical B form of the DNA double-stranded hexadecanucleotide (sequence: ATATCGCGATATCGCG) generated by the 3D-DART server,[58] described by the AMBER ff99 force field,[59] was optimised using the steepest descent method. No cut-offs for electrostatics or van der Waals terms were used due to the small system size; neither the periodic boundary conditions were used nor were the counterions added. Then, a previously optimised model intercalator molecule (tetrapyrido[3,2-*a*:2′,3′-*c*:3″,2″-*h*:2‴,3‴-*j*]phenazine) was inserted either between the 6th and 7th (C,G) base pairs (the "CG" gap) or between the 10th and 11th (A,T) base pairs (the "AT" gap). Such an insertion in the middle of the strand was devised to minimise the boundary effects. The intercalator was described by the GAFF force field, a generalised all-organic companion to the AMBER suite of force fields.[60] The two intercalated structures were then subjected to energy minimisation with the steepest descent procedure. The removal of the intercalator molecule produced two structures with intercalation gaps, used further in the docking studies. The molecular mechanics calculations were carried out with the GROMACS 4.5.5 software.[61]

For the docking analysis we used the AutoDOCK Vina 1.1.2 program,[62] which applies a united-atom scoring function and ignores the user-supplied partial charges. Docking was performed as blind docking (it refers to the use of a box large enough to encompass any possible ligand–receptor interactions) with the set of boxes of 30 × 20 × 30 Å. Other parameters were set as follows: energy range = 10; exhaustiveness = 100. All structures for the docking experiments were prepared using AutoDOCK Tools 1.5.6 A061 and all single bonds in ligands were kept flexible during the experiments. The pictures were prepared using UCSF CHIMERA 1.9[63] and POV-Ray 3.7.[64]

DNA strand break analysis

The ability of **HSf** and its derivatives to induce single- or double-strand breaks in plasmid DNA was tested with the pBR322 plasmid (C = 0.5 mG mL^{-1}). All compounds were dissolved in DMF, whose concentration was kept constant (10% by volume) in the final solution. After 1 h incubation at 42 °C, reaction mixtures (20 μL) were mixed with 3 μL of loading buffer (bromophenol blue in 30% glycerol) and loaded on 1% agarose gels, containing EB, in TBE buffer (90 mM Tris-borate, 20 mM EDTA, pH = 8.0). Gel electrophoresis was performed at a constant voltage of 100 V (4 V cm^{-1}) for 60 min. The gel was photographed and processed with a Digital Imaging System (Syngen Biotech). For the densitometric analysis we used the UltraQuant 6.0 program.

Conclusion

The presented study gives a first insight into the molecular mechanism of cytotoxicity for four new copper(I) complexes (**1-PSf**, **2-PSf**, **3-PSf** and **4-PSf**) with two different diimine ligands (dmp or bq) and phosphine, derived from sparfloxacin – 3rd generation antibiotics. The following four effects were investigated herein and were the trigger points for evaluation of the observed biological activity *in vitro*: (i) the mode of cell death; (ii) intracellular uptake of the tested complexes; (iii) the ability of the complexes to generate reactive oxygen species; and (iv) interactions of complexes with DNA.

(i) All complexes induce apoptosis in prevalence, independently of the cell type and incubation time. The kind of diimine ligand does not exert a meaningful influence on the type of cell death, in contrast to halogen ligands. The iodide ligand induces apoptosis more strongly than the thiocyanate one.

(ii) All copper(I) coordination compounds are characterised by a great capacity to accumulate inside cells. In particular, accumulation of more cytotoxic dmp complexes (**1-PSf**, **2-PSf**) is at a significantly higher level when compared with the bq

(**3-PSf**, **4-PSf**) ones, after the same incubation time. Analyses of the cross-sectional images and emission bands of the cancer cells prove unequivocally that the tested compounds penetrate into the cells. However, there are no favourable locations inside the cell.

(iii) The studied complexes are able to induce ROS generation at a similar level and independently of the type of cell line. Importantly, it was demonstrated that the studied complexes decompose H_2O_2 (free radical mechanism), which can cause additional DNA damage. This confirms that free radicals can be involved in observed cytotoxicity.

(iv) What is noteworthy is that complexes with the bq diimine ligand intercalate to DNA more strongly than the dmp ones, despite the fact that they are less cytotoxic. Moreover, bq complexes induce double-strain plasmid cleavage compared to the dmp ones, which cause only single-strain damage. The results of molecular docking methods show that bq complexes interact with DNA by partial intercalation while dmp complexes do so by groove binding. Presumably, the cytotoxicity of the latter ones is dependent not only on the intercalation to DNA, but also on others' strong interactions with DNA – as was shown by the molecular docking method.

Considering the penetration time and the level of the complexes' accumulation in the cells, the mechanism of their cytotoxicity is probably based mainly on their interactions with DNA. The cytotoxic action mode for dmp complexes is probably different from that for the bq ones. The molecular mechanism of cytotoxicity for **1-PSf** and **2-PSf** is mainly based on: (i) the high level of their accumulation inside cells; (ii) intercalation to DNA molecules; and (iii) other strong interactions such as groove binding. The cytotoxicity mode of action of bq complexes (**3-PSf**, **4-PSf**) can be most likely explained by strong intercalation properties. Their low cytotoxicity is, however, a result of lower accumulation in the cell. This probably means that the bq complexes can interact with cell membranes or other cellular biocomponents. Now we are working on an explanation for this phenomenon. These data require further detailed studies. Finally, it can be claimed that the generation of ROS indirectly contributes to the cytotoxic mechanism of action of all studied complexes.

Acknowledgements

The authors gratefully acknowledge financial support from the Polish National Science Centre (Grant 2011/03/B/ST5/01557). The DFT calculations have been carried out in the Wroclaw Centre for Networking and Supercomputing (http://www.wcss.wroc.pl), grant no. 140. The *in vitro* research was carried out with the equipment purchased thanks to the financial support of the European Regional Development Fund in the Framework of the Polish Innovation Economy Operational Program (contrach no. POIG.02.01.00-12-023/08). The authors are grateful to Bernadeta Nowak. PhD. Jagiellonian University in Kraków for flow cytometry measurements and Mariusz Kępczyński PhD. Jagiellonian University in Kraków for confocal imaging. R.F.M.A. acknowledges funding from F.C.T. Portugal through grant n. UID/MULTI/00612/2013 and IF20102 (POPH, FSE) initiative.

Notes and references

1 C. Santini, M. Pellei, V. Gandin, M. Porchia, F. Tisato and C. Marzano, *Chem. Rev.*, 2014, **114**, 815.
2 G. Borkow and J. Gabbay, *FASEB J.*, 2004, **18**, 1728.
3 J. O. Noyce, H. Michels and C. W. Keevil, *Appl. Environ. Microbiol.*, 2007, **73**, 2748.
4 F. Lebon, N. Boggetto and M. Ledecq, *Biochem. Pharm.*, 2002, **63**, 1863.
5 B. Dudová, D. Hudecová, R. Pokorný, M. Micková, M. Palicová, P. Segĺa and M. Melník, *Folia Microbiol.*, 2002, **47**, 225.
6 E. Weder, C. T. Dillon and T. W. Hambley, *Coord. Chem. Rev.*, 2002, **232**, 95.
7 R. Starosta, A. Bykowska, A. Kyzioł, M. Płotek, M. Florek, J. Król and M. Jeżowska-Bojczuk, *Chem. Biol. Drug Des.*, 2013, **82**, 579.
8 D. Palanimuthu, S. V. Shinde, K. Somasundaram and A. G. Samuelson, *J. Med. Chem.*, 2013, **56**, 722.
9 R. Starosta, A. Brzuszkiewicz, A. Bykowska, U. K. Komarnicka, B. Bażanów, M. Florek, Ł. Gadzała, N. Jackulak, J. Król and K. Marycz, *Polyhedron*, 2013, **50**, 481.
10 V. Gandin, M. Pellei, F. Tisato, M. Porchia, C. Santini and C. Marzano, *J. Cell. Mol. Med.*, 2012, **16**, 142.
11 V. Gandinm, F. Tisato, A. Dolmella, M. Pellei, C. Santini, M. Giorgetti, C. Marzano and M. Porchia, *J. Med. Chem.*, 2014, **57**, 4745.
12 C. Marzano, V. Gandin, M. Pellei, D. Colavito, G. Papini, G. G. Lobbia, E. D. Giudice, M. Porchia, F. Tisato and C. Santini, *J. Med. Chem.*, 2008, **51**, 798.
13 A. Barilli, C. Atzeri, I. Bassanetti, F. Ingoglia, V. Dall'Asta, O. Bussolati, M. Maffini, C. Mucchino and L. Marchiò, *Mol. Pharm.*, 2014, **11**, 1151.
14 S. Tardito, A. Barilli, I. Bassanetti, M. Tegoni, O. Bussolati, R. Franchi-Gazzola, C. Mucchino and L. Marchiò, *J. Med. Chem.*, 2012, **55**, 10448.
15 V. Gandin, M. Porchia, F. Tisato, A. Zanella, E. Severin, A. Dolmella and C. Marzano, *J. Med. Chem.*, 2013, **56**, 7416.
16 X. Wang and Z. Guo, *Chem. Soc. Rev.*, 2013, **42**, 202.
17 N. J. Wheate, S. Walker, G. E. Craig and R. Oun, *Dalton Trans.*, 2010, **39**, 8113.
18 C. Santini, M. Pellei, G. Papini, B. Morresi, R. Galassi, S. Ricci, F. Tisato, M. Porchia, M. P. Rigobello, V. Gandin and C. Marzano, *J. Inorg. Biochem.*, 2011, **105**, 232.
19 R. Galindo-Murillo, J. C. Garcıa-Ramos, L. Ruiz-Azuara, T. E. Cheatham and F. Cortes-Guzm, *Nucleic Acids Res.*, 2015, 1.
20 U. K. Komarnicka, R. Starosta, A. Kyzioł and M. Jeżowska-Bojczuk, *Dalton Trans.*, 2015, **44**, 12688.
21 R. Starosta, U. K. Komarnicka, M. Puchalska and M. Barys, *New J. Chem.*, 2012, **36**, 1673.

22 R. Starosta, U. K. Komarnicka and M. Puchalska, *J. Lumin.*, 2013, **143**, 142.
23 A. Lavie-Cambot, M. Cantuel, Y. Leydet, G. Jonusauskas, D. M. Bassani and N. D. McClenaghan, *Coord. Chem. Rev.*, 2008, **252**, 2572.
24 D. V. Scaltrito, D. W. Thompson, J. A. O'Callaghan and G. J. Meyer, *Coord. Chem. Rev.*, 2000, **208**, 243.
25 K. Folting and L. L. Merritt, *Acta Crystallogr., Sect. B: Struct. Crystallogr. Cryst. Chem.*, 1977, **33**, 3540.
26 N. Fozia, A. Wustholz, R. Kinscherf and N. A. Metzler-Nolte, *Angew. Chem., Int. Ed.*, 2005, **44**, 2429.
27 V. Kalsani, M. Schmittel, A. Listorti, G. Accorsi and N. Armaroli, *Inorg. Chem.*, 2006, **45**, 2061.
28 W. Zhong, J. S. Yu, W. Huang, K. Ni and Y. Liang, *Biopolymers*, 2001, **62**, 315.
29 R. F. Pasternack, E. J. Gibbs and J. J. Villafranca, *Biochemistry*, 1983, **22**, 5409.
30 P. Drevensek, N. Poklar Ulrih, A. Majerle and I. Turel, *J. Inorg. Biochem.*, 2006, **100**, 1705.
31 S. Mahadevan and M. Palaniandavar, *Inorg. Chem.*, 1998, **42**, 693.
32 T. Kloskowski, N. Gurtowska and T. Drewa, *Pulm. Pharmacol. Ther.*, 2010, **23**, 373.
33 O. Azimi, Z. Emami, H. Salari and J. Chamani, *Molecules*, 2011, **16**, 9792.
34 T. Kloskowski, N. Gurtowska, M. Nowak, R. Joachimiak, A. Bajek, J. Olkowska and T. Drewa, *Acta Polym. Pharm.*, 2011, **68**, 859.
35 D. J. Smart, D. Halicka, F. Traganos, Z. Darzynkiewicz and G. M. Williams, *Cancer Biol. Ther.*, 2008, **7**, 113.
36 F. Dimiza, A. N. Papadopoulos, V. Tangoulis, V. Psycharis, C. P. Raptopoulou, D. P. Kessissoglou and G. Psomas, *Dalton Trans.*, 2010, **39**, 4517.
37 W. D. Wilson, L. Ratmeyer, M. Zhao, L. Strekowski and D. Boykin, *Biochemistry*, 1993, **32**, 4098.
38 G. Zhao, H. Lin, S. Zhu, H. Sun and Y. Chen, *J. Inorg. Biochem.*, 1998, **70**, 219.
39 E. Nordmeier, *J. Phys. Chem.*, 1992, **96**, 6045.
40 A. Tarushi, E. Polatoglou, J. Kljun, I. Turel, G. Psomas and D. P. Kessissoglou, *Dalton Trans.*, 2011, **40**, 9461.
41 K. C. Skyrianou, V. Psycharis, C. P. Raptopoulou, D. P. Kessissoglou and G. Psomas, *J. Inorg. Biochem.*, 2011, **105**, 63.
42 K. C. Skyrianou, F. Perdih, A. N. Papadopoulos, I. Turel, D. P. Kessissoglou and G. Psomas, *J. Inorg. Biochem.*, 2011, **105**, 1273.
43 K. Jeyalakshmi, Y. Arun, N. S. P. Bhuvanesh, P. T. Perumal, A. Sreekanth and R. Karvembu, *Inorg. Chem. Front.*, 2015, **2**, 780.
44 A. Coutinho and M. Prieto, *J. Chem. Educ.*, 1993, **70**, 425.
45 T. Jia, J. Wang, P. Yu and J. Guo, *Org. Biomol. Chem.*, 2015, **13**, 1234.
46 H. Rozenberg, D. Rabinovich, F. Frolow, R. S. Hegde and Z. Shakked, *Proc. Natl. Acad. Sci. U. S. A.*, 1998, **95**, 15194.
47 A. Bykowska, R. Starosta, J. Jezierska and M. Jeżowska-Bojczuk, *RSC Adv.*, 2015, **5**, 80804.
48 K. Manojkumar, K. T. P. Charan, A. Sivaramakrishna, P. C. Jha, V. M. Khedkar, R. Siva, G. Jayaraman and K. Vijayakrishna, *Biomacromolecules*, 2015, **16**, 894.
49 U. K. Komarnicka, R. Starosta, K. Guz-Regner, G. Bugla-Płoskońska, A. Kyzioł and M. Jeżowska-Bojczuk, *J. Mol. Struct.*, 2015, **1096**, 55.
50 R. K. Ralph, B. Marshall and S. Darkin, *Trends Biochem. Sci.*, 1983, **8**, 212.
51 W. Szczepanik, P. Kaczmarek and M. Jeżowska-Bojczuk, *J. Inorg. Biochem.*, 2004, **98**, 2141.
52 A. R. Kennedy and M. C. Symons, *Carcinogenesis*, 1987, **8**, 683.
53 L. Becco, A. Rodríguez, M. E. Bravo, M. J. Prieto, L. Ruiz-Azuara, B. Garat, V. Moreno and D. Gambino, *J. Inorg. Biochem.*, 2012, **109**, 49.
54 M. J. Frisch, G. W. Trucks, H. B. Schlegel, G. E. Scuseria, M. A. Robb, J. R. Cheeseman, G. Scalmani, V. Barone, B. Mennucci, G. A. Petersson, H. Nakatsuji, M. Caricato, X. Li, H. P. Hratchian, A. F. Izmaylov, J. Bloino, G. Zheng, J. L. Sonnenberg, M. Hada, M. Ehara, K. Toyota, R. Fukuda, J. Hasegawa, M. Ishida, T. Nakajima, Y. Honda, O. Kitao, H. Nakai, T. Vreven, J. A. Montgomery Jr., J. E. Peralta, F. Ogliaro, M. Bearpark, J. J. Heyd, E. Brothers, K. N. Kudin, V. N. Staroverov, T. Keith, R. Kobayashi, J. Normand, K. Raghavachari, A. Rendell, J. C. Burant, S. S. Iyengar, J. Tomasi, M. Cossi, N. Rega, J. M. Millam, M. Klene, J. E. Knox, J. B. Cross, V. Bakken, C. Adamo, J. Jaramillo, R. Gomperts, R. E. Stratmann, O. Yazyev, A. J. Austin, R. Cammi, C. Pomelli, J. W. Ochterski, R. L. Martin, K. Morokuma, V. G. Zakrzewski, G. A. Voth, P. Salvador, J. J. Dannenberg, S. Dapprich, A. D. Daniels, O. Farkas, J. B. Foresman, J. V. Ortiz, J. Cioslowski and D. J. Fox, *Gaussian 09, Revision D.01*, Gaussian, Inc., Wallingford, CT, 2013.
55 Y. Zhao and D. G. Truhlar, *Theor. Chem. Acc.*, 2008, **120**, 215.
56 D. Feller, *J. Comput. Chem.*, 1996, **17**, 1571.
57 K. L. Schuchardt, B. T. Didier, T. Elsethagen, L. Sun, V. Gurumoorthi, J. Chase, J. Li and T. L. Windus, *J. Chem. Inf. Model.*, 2007, **47**, 1045.
58 van M. Dijk and A. M. J. J. Bonvin, *Nucleic Acids Res.*, 2009, **37**, 235.
59 M. Wang, P. Cieplak and P. A. Kollman, *J. Comput. Chem.*, 2000, **21**, 1049.
60 J. Wang, R. M. Wolf, J. W. Caldwell, P. A. Kollman and D. A. Case, *J. Comput. Chem.*, 2004, **25**, 1157.
61 S. Pronk, S. Páll, R. Schulz, P. Larsson, P. Bjelkmar, R. Apostolov, M. R. Shirts, J. C. Smith, P. M. Kasson, D. van der Spoel, B. Hess and E. Lindahl, *Bioinformatics*, 2013, **29**, 845.
62 O. Trott and A. J. Olson, *J. Comput. Chem.*, 2010, **31**, 455.
63 F. Pettersen, T. D. Goddard, C. C. Huang, G. S. Couch, D. M. Greenblatt, E. C. Meng and T. E. Ferrin, *J. Comput. Chem.*, 2004, **25**, 1605.
64 *POV-Ray for Windows, version 3.7.0.msvc0.win64* (http://www.povray.org).

